



Since January 2020 Elsevier has created a COVID-19 resource centre with free information in English and Mandarin on the novel coronavirus COVID-19. The COVID-19 resource centre is hosted on Elsevier Connect, the company's public news and information website.

Elsevier hereby grants permission to make all its COVID-19-related research that is available on the COVID-19 resource centre - including this research content - immediately available in PubMed Central and other publicly funded repositories, such as the WHO COVID database with rights for unrestricted research re-use and analyses in any form or by any means with acknowledgement of the original source. These permissions are granted for free by Elsevier for as long as the COVID-19 resource centre remains active.



# A high-affinity aptamer with base-appended base-modified DNA bound to isolated authentic SARS-CoV-2 strains wild-type and B.1.617.2 (delta variant)



Hiroataka Minagawa<sup>a</sup>, Hirofumi Sawa<sup>b, c, d, \*</sup>, Tomoko Fujita<sup>a</sup>, Shintaro Kato<sup>a</sup>, Asumi Inaguma<sup>a</sup>, Miwako Hirose<sup>a</sup>, Yasuko Orba<sup>b, c</sup>, Michihito Sasaki<sup>b</sup>, Koshiro Tabata<sup>b</sup>, Naoki Nomura<sup>e</sup>, Masashi Shingai<sup>c, e</sup>, Yasuhiko Suzuki<sup>f</sup>, Katsunori Horii<sup>a, \*\*</sup>

<sup>a</sup> NEC Solution Innovators, Ltd., 1-18-7, Shinkiba, Koto-ku, Tokyo, 136-8627, Japan

<sup>b</sup> Division of Molecular Pathobiology, International Institute for Zoonosis Control, Hokkaido University, N20, W10, Kita-ku, Sapporo, 001-0020, Japan

<sup>c</sup> International Collaboration Unit, International Institute for Zoonosis Control, Hokkaido University, N20, W10, Kita-ku, Sapporo, 001-0020, Japan

<sup>d</sup> One Health Research Center, Hokkaido University, N20, W10, Kita-ku, Sapporo, 001-0020, Japan

<sup>e</sup> Laboratory for Biologics Development, International Institute for Zoonosis Control, Hokkaido University, N20, W10, Kita-ku, Sapporo, 001-0020, Japan

<sup>f</sup> Division of Bioresource, International Institute for Zoonosis Control, Hokkaido University, N20, W10, Kita-ku, Sapporo, 001-0020, Japan

## ARTICLE INFO

### Article history:

Received 5 April 2022

Accepted 15 April 2022

Available online 2 May 2022

### Keywords:

Base-appended base aptamer  
Severe acute respiratory syndrome coronavirus 2 (SARS-CoV-2)  
Variants  
Spike glycoprotein  
Receptor-binding domain  
Enzyme-linked aptamer assay

## ABSTRACT

Simple, highly sensitive detection technologies for severe acute respiratory syndrome coronavirus 2 (SARS-CoV-2) are crucial for the effective implementation of public health policies. We used the systematic evolution of ligands by exponential enrichment with a modified DNA library, including a base-appended base (uracil with a guanin base at its fifth position), to create an aptamer with a high affinity for the receptor-binding domain (RBD) of the SARS-CoV-2 spike glycoprotein. The aptamer had a dissociation constant of 1.2 and < 1 nM for the RBD and spike trimer, respectively. Furthermore, enzyme-linked aptamer assays confirmed that the aptamer binds to isolated authentic SARS-CoV-2 wild-type and B.1.617.2 (delta variant). The binding signal was larger than that of commercially available anti-SARS-CoV-2 RBD antibody. Thus, this aptamer as a sensing element will enable the highly sensitive detection of SARS-CoV-2.

© 2022 Elsevier Inc. All rights reserved.

## 1. Introduction

Severe acute respiratory syndrome coronavirus 2 (SARS-CoV-2), the cause of the novel coronavirus disease-2019 (COVID-19) pandemic, triggers acute respiratory diseases, and the COVID-19 pandemic is a global threat to public health [1]. Recently, one of

the variants of concern (VoCs), B.1.617.2 (delta variant) has spread rapidly all over the world. SARS-CoV-2 mainly infects human alveolar epithelial cells by binding to angiotensin-converting enzyme 2 via the receptor-binding domain (RBD) of the spike (S) protein, a surface glycoprotein on the viral particle [2,3]. Therefore, the S protein is an important target for detecting SARS-CoV-2 as well as developing antiviral antibodies and compounds [4].

Antibodies, which bind specifically to target proteins, are widely used in research and therapeutics. For example, a lateral flow assay has been developed using antibodies against SARS-CoV-2 [5,6]. Antibodies are the gold standard for recognizing molecules; however, they have drawbacks, including instability and high costs of development and production [7].

Aptamers are single-stranded DNA (ssDNA) or RNA oligonucleotides that bind to specific molecules or cells [8,9]. Therefore, aptamers are able to regulate the functions of the targets similarly as antibodies. Additionally, aptamers have some advantages, such as easiness of both efficient production and chemical modification,

\* Corresponding author. Division of Molecular Pathobiology, International Institute for Zoonosis Control, Hokkaido University, N20, W10, Kita-ku, Sapporo, 001-0020, Japan.

\*\* Corresponding author. NEC Solution Innovators, Ltd., 1-18-7, Shinkiba, Koto-ku, Tokyo, 136-8627, Japan.

E-mail addresses: [minagawa-hir@nec.com](mailto:minagawa-hir@nec.com) (H. Minagawa), [h-sawa@czc.hokudai.ac.jp](mailto:h-sawa@czc.hokudai.ac.jp) (H. Sawa), [tom-fujita@nec.com](mailto:tom-fujita@nec.com) (T. Fujita), [katou-s-mxn@nec.com](mailto:katou-s-mxn@nec.com) (S. Kato), [a\\_inaguma@nec.com](mailto:a_inaguma@nec.com) (A. Inaguma), [m-hirose-ys@nec.com](mailto:m-hirose-ys@nec.com) (M. Hirose), [orbay@czc.hokudai.ac.jp](mailto:orbay@czc.hokudai.ac.jp) (Y. Orba), [m-sasaki@czc.hokudai.ac.jp](mailto:m-sasaki@czc.hokudai.ac.jp) (M. Sasaki), [k-tabata@czc.hokudai.ac.jp](mailto:k-tabata@czc.hokudai.ac.jp) (K. Tabata), [nomura@czc.hokudai.ac.jp](mailto:nomura@czc.hokudai.ac.jp) (N. Nomura), [shingaim@czc.hokudai.ac.jp](mailto:shingaim@czc.hokudai.ac.jp) (M. Shingai), [suzuki@czc.hokudai.ac.jp](mailto:suzuki@czc.hokudai.ac.jp) (Y. Suzuki), [k-horii@nec.com](mailto:k-horii@nec.com) (K. Horii).

### Abbreviations

Severe acute respiratory syndrome coronavirus 2 SARS-CoV-2  
 systematic evolution of ligands by exponential enrichment SELEX  
 base-appended base BAB  
 receptor-binding domain RBD  
 selection buffer SB  
 forward Fw  
 reverse Rv  
 double-stranded DNA dsDNA  
 single-stranded DNA ssDNA  
 surface plasmon resonance SPR  
 enzyme-linked aptamer assay ELAA  
 fast string-based clustering FSBC

and reversible folding without aggregation [10–12].

Aptamers are usually isolated from combinatorial nucleic acid libraries using an iterative selection process called systematic evolution of ligands by exponential enrichment (SELEX) [13]. The SELEX method uses a library comprising primer regions and random regions to select the sequences binding to the target [14,15]. We have developed analogs with modified bases containing other bases, i.e., base-appended bases (BABs). Using these modified bases, we have generated aptamers with extremely high binding affinities for various targets [22–25].

Aptamers for SARS-CoV-2 S protein or RBD have been selected from a DNA library using natural bases [16,17]. Also, an aptamer inhibiting SARS-CoV-2 infection has been identified [18–21]. In this study, a high-affinity artificial nucleic acid aptamer for the SARS-CoV-2 S RBD was obtained using a modified DNA library containing the following base-appended base modifications; analog guanine derivative at the fifth position of uracil ( $U^{gu}$ ) [23]. This aptamer was shown to detect authentic SARS-CoV-2 strains belonging to lineages A and B.1.617.2.

## 2. Materials and methods

### 2.1. Target protein and virus

The recombinant RBD of the SARS-CoV-2 (2019-nCoV) S protein (YP\_009724390.1, Arg319-Phe541) and the His-tagged S1+S2 ECD protein (YP\_009724390.1, Val16-Pro1213) (Sino Biological, Beijing, China) were used as the selection targets.

All the experiments using SARS-CoV-2 were performed under the guidelines of the Biosafety Management Committee on Pathogens and Other Hazardous Agents of Hokkaido University and the International Institute for Zoonosis Control. SARS-CoV-2 strains belonging to lineages A [26], B.1.1.7 (alpha variant), B.1.351 (beta variant), P.1 (gamma variant), B.1.617.2 (delta variant), and human coronavirus OC43 (HCoV-OC43) were prepared separately. Those SARS-CoV-2 strains were isolated and provided by Drs. Saijyo and Shimojima at the National Institute of Infectious Diseases, Tokyo, Japan. First, each strain of SARS-CoV-2 was inoculated into Vero-TMPRSS2 cells [27] cultured in Dulbecco's modified Eagle's medium containing 2% fetal bovine serum, and the supernatants were collected upon observation of cytopathic effects. Meanwhile, HCoV-OC43 was inoculated into MRC-5 cells, and the supernatants were collected in the same manner. Then, the viruses were pelleted by ultracentrifugation at  $110,000\times g$  at  $4^\circ C$  for 2 h with a 20% sucrose cushion. Afterward, the pellets were resuspended in phosphate-buffered saline (PBS) and

stored at  $-80^\circ C$ . Viral titers were measured by plaque assays [27].

### 2.2. SELEX

SELEX was conducted as previously reported [23]. Dynabeads MyOne Carboxylic Acid and Dynabeads MyOne SA C1 magnetic beads (Invitrogen, Waltham, MA) were used for target solidification and biotinylated DNA retrieval, respectively. The target beads were prepared by binding MyOne Carboxylic Acid to recombinant RBD according to the manufacturer's instructions and washed with the selection buffer [SB; 40 mM HEPES (pH 7.5), 125 mM NaCl, 5 mM KCl, 1 mM  $MgCl_2$ , and 0.01% Tween 20]. A double-stranded DNA (dsDNA) with inserted  $U^{gu}$  was prepared using a 5'-biotin-modified complementary strand (5'-GAATACAAGACACCTCGGCTTTGC-N30-GATTCAGTGGCGGAGACATAACC-3'), a forward (Fw) primer (5'-GGTATGCTCCGCCACTGAAATC-3'), and KOD Dash (Toyobo, Osaka, Japan). After the dsDNA was bound to MyOne SA C1 magnetic beads, ssDNA was eluted with 0.02 M NaOH and neutralized with 0.08 M HCl to prepare the  $U^{gu}$  ssDNA library. The primers, random pool, and aptamer clone templates were purchased from Integrated DNA Technologies (Tokyo, Japan).

The 130 pmol library was mixed for 15 min with 250  $\mu g$  of target beads at  $25^\circ C$ . Then, the beads were washed with SB, and the bound ssDNA was eluted with 7 M urea and amplified by polymerase chain reaction (PCR) using the Fw primer and a reverse (Rv) primer (5'-GAATACAAGACACCTCGGCTTTGC-3') with modification by the 5'-biotin. Next, the amplified dsDNA was bound to MyOne SA C1 magnetic beads, and the Fw chain was eluted with 0.02 M NaOH. The ssDNA produced by this method, using the Rv chain, Fw primer, and  $U^{gu}$ -immobilized in magnetic beads, were used in the next round. After eight rounds of selection, PCR with the Fw and Rv primers and subsequent sequencing were conducted using a MiniSeq System (Illumina, San Diego, CA). The sequence data obtained were clustered by fast string-based clustering (FSBC), and 1 sequence each was selected from the top and another higher-ranked clusters [28].

### 2.3. Surface plasmon resonance analysis

All the surface plasmon resonance (SPR) measurements were performed at  $25^\circ C$  using the ProteON XPR360 (Bio-Rad, Hercules, CA) [22]. For the aptamer clones, the ligand was set by appending poly- $A_{20}$  at the 3'-end and hybridizing the 5'-end to an NLC sensor chip (Bio-Rad) with biotin-modified oligo ( $dT_{20}$ ) [23]. The analytes included the RBD, S1+S2, recombinant 2019-nCoV S1 (Elabscience, Houston, TX), and recombinant 2019-nCoV S trimers (Elabscience). Bovine serum albumin (Sigma-Aldrich, St. Louis, MO) with SB was used as the running buffer. The dissociation constants between the aptamer and recombinant RBD or S protein were calculated using a simple 1:1 biomolecular interaction model, the most common kinetic fit model for SPR data analysis, according to the manufacturer's instructions. The dissociation constant of S protein was estimated as the apparent  $K_d$  value due to its trimeric formation.

### 2.4. Enzyme-linked aptamer assays

Enzyme-linked aptamer assays (ELAAs) were conducted as previously described [29]. Briefly, recombinant RBD protein and purified SARS-CoV-2 were diluted with 50 mM carbonate buffer (pH 9.6), added to MaxiSorp plates (Thermo Scientific, Waltham, MA), at 1  $\mu g$ /well and  $1.0 \times 10^6$  PFU/well, respectively, and solidified at  $4^\circ C$  overnight. Recombinant His-tagged hemagglutinin (HA) protein of influenza A/California/04/2009H1N1 (Sino Biological, Beijing, China) was used as a negative control. Then, the wells were washed once with SB and blocked with Tris-buffered saline

Blocking Buffer (Pierce Biotechnology, Rockford, IN) at 25 °C for 1 h. Then, a 5' biotinylated aptamer at 1 μM was prepared in SB, denatured by heating at 95 °C for 5 min, and cooled. Next, the aptamer was added and incubated at room temperature for 1 h. After three washes with SB, streptavidin–horseradish peroxidase (HRP) (1:1,000 diluted; Citiva, New York, NY) was added, and the plates were incubated for 30 min at room temperature to detect the bound biotinylated aptamers. After three washes with SB, a 3,3',5,5'-Tetramethylbenzidine (TMB) solution (Thermo Fisher Scientific) for RBD detection and 1-step™ Ultra TMB-ELISA substrate solution (Thermo Fisher Scientific) for SARS-CoV-2 detection was added, and the plates were incubated at room temperature for 10 min. The reaction was stopped by adding 0.5 N sulfuric acid, and the absorbance was measured at 450, 490 and 620 nm.

### 2.5. Statistical analysis

All statistical analyses were performed using R version 4.0.4. For analyses between two groups, a one-tailed Student's unpaired *T*-test was applied. For comparisons among more than two groups, one-way ANOVA with Tukey's multiple comparisons was used. The methods of statistical analysis are described in the figure legends for each experiment.

## 3. Results and discussion

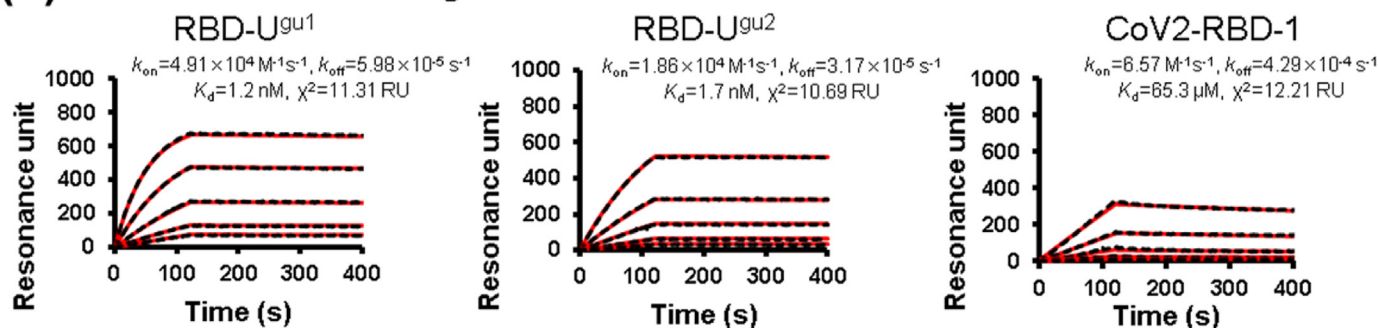
For the detection of SARS-CoV-2, the S protein-binding aptamers were screened using a U<sup>gu</sup>-modified nucleic acid library. Four S protein-binding aptamers candidates [28], two for the RBD and two for the S1+S2 protein (Table S1), were selected from sequence

analysis. Four analytes, S1 and S trimers in addition to RBD and S1+S2, were used for SPR analysis. The two RBD-binding aptamers, RBD-U<sup>gu1</sup> and RBD-U<sup>gu2</sup>, bound all four analytes. However, the two S1+S2-binding aptamers, S1S2-U<sup>gu3</sup> and S1S2-U<sup>gu4</sup>, failed to bind the RBD (Fig. S1).

The RBD-binding ability of a previously reported aptamer, CoV2-RBD-1 [16], was compared with that of RBD-U<sup>gu1</sup> and RBD-U<sup>gu2</sup> using SPR analysis. The dissociation constants of RBD-U<sup>gu1</sup> and RBD-U<sup>gu2</sup> were 1.2 and 1.7 nM, respectively, demonstrating more strong binding affinities than CoV2-RBD-1 (Fig. 1a). In a solution containing dextran sulfate, a polyanion suppressing nonspecific binding to nucleic acids [30,31], CoV2-RBD-1 significantly lost its binding activity. Conversely, the dissociation constants for RBD-U<sup>gu1</sup> and RBD-U<sup>gu2</sup> were 3.2 and 3.5 nM, respectively, indicating that their binding activities remained largely unaffected (Fig. 1b). This observation suggests that charge has little influence on the ability of RBD-U<sup>gu1</sup> and RBD-U<sup>gu2</sup> to bind RBD, even though the binding of aptamers to the target is usually influenced by charge. These data indicate that RBD-U<sup>gu1</sup> and RBD-U<sup>gu2</sup> exhibit little nonspecific binding. Additionally, the evaluation of the binding of RBD-U<sup>gu1</sup> and RBD-U<sup>gu2</sup> to the S trimer using SPR revealed a dissociation constant of less than 1 nM for both aptamers, indicating exceptionally strong binding (Fig. S2). The binding sites on RBD for RBD-U<sup>gu1</sup> and RBD-U<sup>gu2</sup> are unclear. Since BAB clones have different structures from natural-base clones with corresponding sequences (in which dU<sup>x</sup> is dT) [22], the more complex structures of RBD-U<sup>gu1</sup> and RBD-U<sup>gu2</sup> may result in stronger RBD binding.

Generally, a longer sequence results in the instability of an aptamer's conformation at the interface of the target [32]. Hence, the length of aptamers should be minimized to enhance the

### (a) SB was used as running buffer



### (b) SB with 0.1% dextran sulfate was used as running buffer

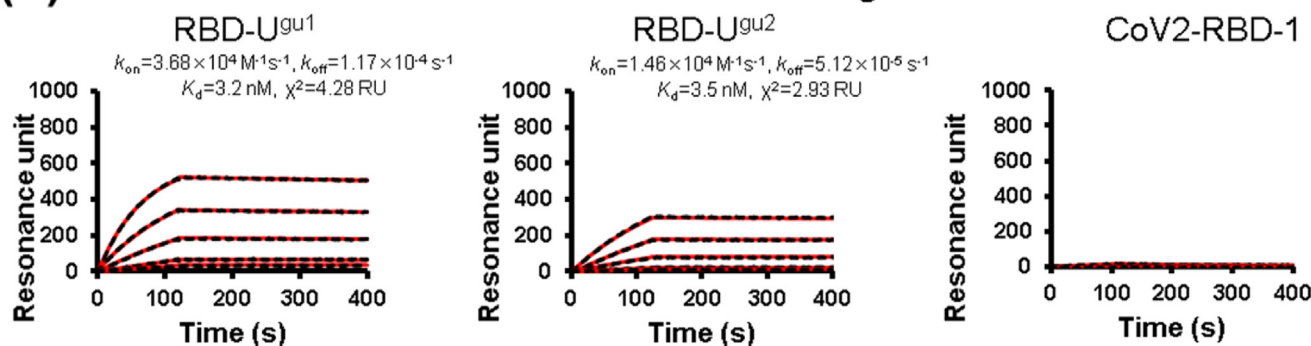


**Fig. 1.** SPR response curves of the interaction between the SARS-CoV-2 S RBD and the aptamer candidates, RBD-U<sup>gu1</sup>, RBD-U<sup>gu2</sup>, and CoV2-RBD-1

(a–b) Different concentrations of RBD (25–400 nM) were injected over the respective aptamer-immobilized sensor chips for 120 s at a flow rate of 50 μL/min, and the measurements were performed using multicycle kinetics. Black dot line and red line represent the measured and fitting curves, respectively. The average of the squared differences between the data points and the corresponding fitted values is represented as  $\chi^2$ . (For interpretation of the references to colour in this figure legend, the reader is referred to the Web version of this article.)

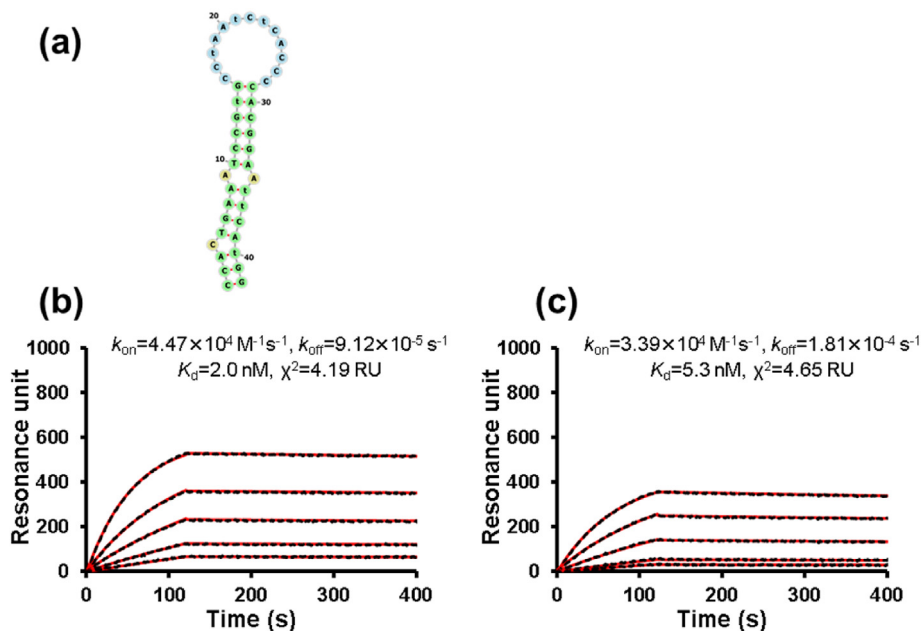


**Fig. 2.** Properties of the truncated RBD-U<sup>gu1-1</sup> aptamer

(a) The predicted secondary structure of RBD-U<sup>gu1-1</sup> which was estimated with RNAfold of ViennaRNA package [34] was displayed using Forna [37]. (b–c) The SPR response curves of the interaction between SARS-CoV-2 S RBD protein and RBD-U<sup>gu1-1</sup>. Black dot line and red line represent the measured and fitting curves, respectively. The average of the squared differences between the measured data points and the corresponding fitted values is represented as  $\chi^2$ . In (b), SB was used as a running buffer; in (c), SB with 0.1% dextran sulfate was used. (For interpretation of the references to colour in this figure legend, the reader is referred to the Web version of this article.)

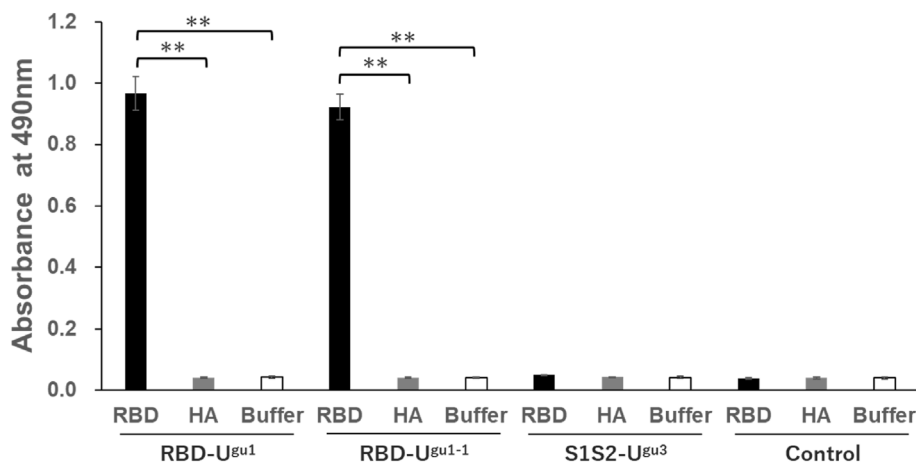


**Fig. 3.** Binding capacities of RBD-U<sup>gu1</sup>, RBD-U<sup>gu1-1</sup>, and S1S2-U<sup>gu3</sup> to the RBD of the spike protein and HA protein derived from influenza H1N1 virus as measured by direct ELAA. The amount of the 5' biotinylated aptamer captured by immobilized RBD and HA was determined the absorbance at 490 nm. The experiment was performed in triplicates. Error bars represent standard deviation for 6 data points. Buffer was used Selection Buffer [40 mM HEPES (pH 7.5), 125 mM NaCl, 5 mM KCl, 1 mM MgCl<sub>2</sub>, and 0.01% Tween 20]. One-tailed unpaired *T*-test was applied to compare the mean of ELAA signals of the RBD with that of HA protein or buffer for each aptamer. The symbol of two asterisks stands for *P* value less than 0.01.

aptamers' binding ability and reduce their cost of production [33]. We designed a truncated aptamer sequence (RBD-U<sup>gu1-1</sup>) with the region in RBD-U<sup>gu1</sup> most strongly related to binding (5'-GGAATTCATG-3'), which was estimated with FSBC, considering the maintenance of the secondary structure of the binding region. RBD-U<sup>gu1-1</sup> was a 42-mer with the sequence of 5'-CCACTGAAATCCGtGCC-tAAtCtCACCCACGGAAAtCAtGG-3', with t indicating U<sup>gu</sup>. The secondary structure of RBD-U<sup>gu1-1</sup> was predicted with RNAfold of ViennaRNA package [34] (Fig. 2a). The dissociation constant of RBD-U<sup>gu1-1</sup> for RBD was 2 nM in SB (Fig. 2b) and 5.3 nM in dextran sulfate (Fig. 2c), exhibiting a binding ability comparable with that of the original sequence. Next, a direct ELAA was conducted using the 5'-terminal biotinylated aptamers to the recombinant RBD proteins

and various SARS-CoV-2 strains immobilized on 96-well plates. RBD-U<sup>gu1</sup> and RBD-U<sup>gu1-1</sup> bound equally well to the RBD. However, S1S2-U<sup>gu3</sup> did not bind to the RBD (Fig. 3). These results were consistent with those of the SPR binding assays. No binding signal of aptamers to influenza virus HA protein was detected, suggesting that aptamers specifically recognize spike proteins of SARS-CoV-2.

Then, the ability of RBD-U<sup>gu1-1</sup> to detect authentic SARS-CoV-2 was evaluated with SARS-CoV-2 lineages A, B.1.617.2, B.1.1.7, B.1.351 and P.1 using direct ELAA (Fig. 4). As a control, a commercially available anti-SARS-CoV-2-RBD antibody conjugated with HRP (Abcam, Cambridge, UK) was used with 1:1,000 dilution. The aptamer was bound to authentic SARS-CoV-2 wild-type and B.1.617.2 immobilized on a plate (Fig. 4a). The binding signals of the

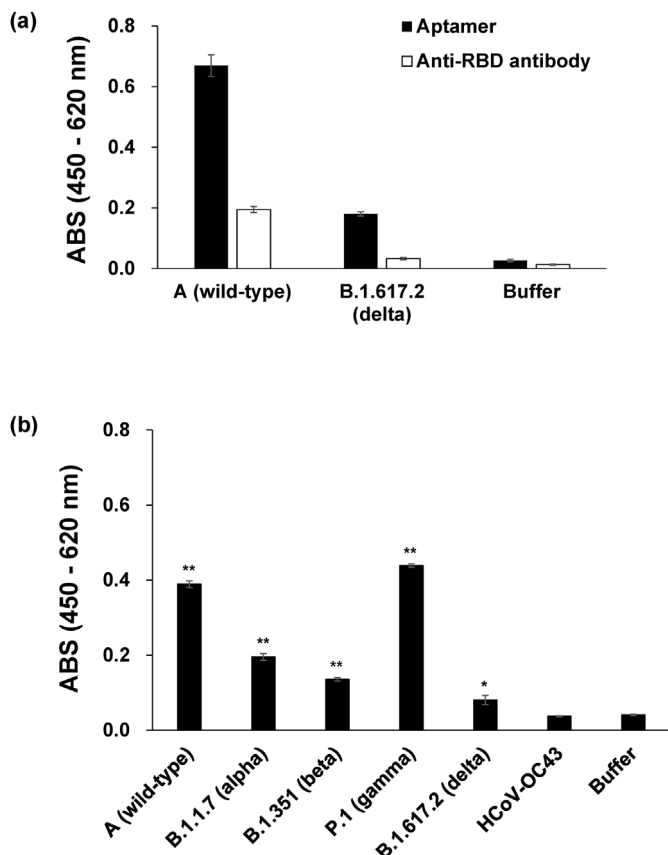


**Fig. 4.** Binding capacities of RBD-U<sup>gu1-1</sup> aptamer to SARS-CoV-2 strains as measured by direct ELAA

(a) The amount of the 5'-biotinylated aptamer and an anti-SARS-CoV-2 RBD antibody captured by immobilized SARS-CoV-2 strains lineage A (wild-type) and B.1.617.2 (delta variant) was determined using SA-HRP and TMB substrate. The absorbance was determined by subtracting the absorbance at 620 nm from that at 450 nm. The experiment was repeated twice with each data point measured in triplicates. Error bars represent standard error. Selection Buffer [40 mM HEPES (pH 7.5), 125 mM NaCl, 5 mM KCl, 1 mM MgCl<sub>2</sub>, and 0.01% Tween 20] was used as a negative control.

(b) The amount of the 5'-biotinylated aptamer captured by immobilized SARS-CoV-2 strains ( $1.0 \times 10^6$  PFU), including lineage A (wild-type), B.1.1.7 (alpha variant), P.1 (gamma variant), B.1.617.2 (delta variant) of SARS-CoV-2 and HCoV-OC43 was determined in the SB containing 0.1% dextran sulfate using SA-HRP and TMB substrate. The absorbance was measured at 450–620 nm. The experiment was repeated twice with each data point measured in triplicates. Error bars represent standard error. One-tailed unpaired *T*-test was applied to compare the mean of ELAA signals between each strain and buffer [SB; 40 mM HEPES (pH 7.5), 125 mM NaCl, 5 mM KCl, 1 mM MgCl<sub>2</sub>, and 0.01% Tween 20]. Double asterisks (\*\*) indicate  $p < 0.01$ ; single asterisk (\*) indicates  $p < 0.05$ . For multiple comparisons between SARS-CoV-2 strains, one-way ANOVA with Tukey's multiple comparisons was used.

aptamer to SARS-CoV-2 wild-type and B.1.617.2 were higher than that of the antibody, indicating that this aptamer has a potential as a better alternative for SARS-CoV-2 detection. The aptamer binding signals to B.1.1.7, B.1.351, and B.1.617.2 are reduced compared with that of wild-type at a significance level of 5%, suggesting that some mutations of these variant affect the aptamer binding. The binding signal to B.1.617.2 is the lowest between them. The mutations introduced in RBD are only two residues, L452R and T478K (<https://www.ecdc.europa.eu/en/covid-19/variants-concern>). Residue 452 is located in a "hull" portion, while residue 478 is located in the outer loop region (PDB entry number: 6m0j, [35]). Based on the modeling results of previous report [36], the replacement of residue 452 may cause to reduce the aptamer binding by steric effect or re-arrangement of the small beta-sheet. Even though the aptamer binding signal to B.1.617.2 is decreased slightly compared

to wild-type, it was able to bind all examined variants of SARS-CoV-2 and not to HCoV-OC43 at all that has distinct RBD (Fig. 4b). Hence, this aptamer has a potential to bind to RBD of SARS-CoV-2 strains with high specificity.

In conclusion, we have demonstrated that synthesized aptamers by BAB modification, RBD-U<sup>gu1</sup> and RBD-U<sup>gu1-1</sup>, efficiently bind with recombinant SARS-CoV-2 S protein and authentic SARS-CoV-2 strains, including wild-type and B.1.617.2, suggesting that these aptamers may be a useful tool for detecting SARS-CoV-2 in the environment.

#### Declaration of competing interest

This work was partly supported by grants for the Japan Program for Infectious Diseases Research and Infrastructure (JP21wm0225003 and JP21fk0108104j) from Japan Agency for Medical Research and Development (AMED) and fund from NEC Solution Innovators, Ltd.

#### Acknowledgements

We thank Drs. Saijyo, Shimojima and Ito at the National Institute of Infectious Diseases, Japan for providing SARS-CoV-2 lineages A, B.1.617.2, B.1.1.7, B.1.351 and P.1 strains. This work was partly supported by grants for the Japan Program for Infectious Diseases Research and Infrastructure (JP21wm0225003 and JP21fk0108104) from Japan Agency for Medical Research and Development (AMED).

#### Appendix A. Supplementary data

Supplementary data to this article can be found online at <https://doi.org/10.1016/j.bbrc.2022.04.071>.

#### References

- [1] Coronaviridae Study Group of the International Committee on Taxonomy of Viruses, The species severe acute respiratory syndrome-related coronavirus: classifying, nCoV and naming it SARS-CoV-2, *Nat. Microbiol.* 4 (2020) 536–544, 2019.
- [2] A.C. Walls, Y.J. Park, M.A. Tortorici, A. Wall, A.T. McGuire, D. Velesler, Structure, function, and antigenicity of the SARS-CoV-2 spike glycoprotein, *Cell* 181 (2020) 281–292, <https://doi.org/10.1016/j.cell.2020.02.058>, e6.
- [3] R. Yan, Y. Zhang, Y. Li, L. Xia, Y. Guo, Q. Zhou, Structural basis for the recognition of SARS-CoV-2 by full-length human ACE2, *Science* 367 (2020) 1444–1448, <https://doi.org/10.1126/science.abb2762>.
- [4] D. Wrapp, N. Wang, K.S. Corbett, J.A. Goldsmith, C.L. Hsieh, O. Abiona, B.S. Graham, J.S. McLellan, Cryo-EM structure of the 2019-nCoV spike in the prefusion conformation, *Science* 367 (2020) 1260–1263, <https://doi.org/10.1126/science.abb2507>.
- [5] B.D. Grant, C.E. Anderson, J.R. Williford, L.F. Alonzo, V.A. Glukhova, D.S. Boyle, B.H. Weigl, K.P. Nichols, SARS-CoV-2 coronavirus nucleocapsid antigen-detecting half-strip lateral flow assay toward the development of point of care tests using commercially available reagents, *Anal. Chem.* 92 (2020) 11305–11309, <https://doi.org/10.1021/acs.analchem.0c01975>.
- [6] L. Azzi, A. Baj, T. Alberio, M. Lualdi, G. Veronesi, G. Carcano, W. Ageno, C. Gambarini, L. Maffioli, S.D. Saverio, D.D. Gasperina, A.P. Genoni, E. Premi, S. Donati, C. Azzolini, A.M. Grandi, F. Dentali, F. Tangianu, F. Sessa, V. Maurino, L. Tettamanti, C. Siracusa, A. Vigezzi, E. Monti, V. Iori, D. Iovino, G. Ietto, ASST dei Sette Laghi Rapid Salivary Test Nurse staff Research Group, P.A. Grossi, A. Tagliabue, M. Fasano, Rapid Salivary Test suitable for a mass screening program to detect SARS-CoV-2: a diagnostic accuracy study, *J. Infect.* 81 (2020) e75–e78, <https://doi.org/10.1016/j.jinf.2020.06.042>.
- [7] C. Ellen, J. N. Blake, *Electrochemical biosensors for pathogen detection*, *Biosens. Bioelectron.* 159 (2020) 112214.
- [8] A.D. Ellington, J.W. Szostak, In vitro selection of RNA molecules that bind specific ligands, *Nature* 346 (1990) 818–822, <https://doi.org/10.1038/346818a0>.
- [9] C. Tuerk, L. Gold, Systematic evolution of ligands by exponential enrichment: RNA ligands to bacteriophage T4 DNA polymerase, *Science* 249 (1990) 505–510, <https://doi.org/10.1126/science.2200121>.
- [10] F. Odeh, H. Nsairat, W. Alshaer, M.A. Ismail, E. Esawi, B. Qaqish, A.A. Bawab, S.I. Ismail, Aptamers chemistry: chemical modifications and conjugation strategies, *Molecules* 25 (2019) 3, <https://doi.org/10.3390/molecules25010003>.

- [11] V. Crivianu-Gaita, M. Thompson, Aptamers, antibody scFv, and antibody Fab' fragments: an overview and comparison of three of the most versatile biosensor biorecognition elements, *Biosens. Bioelectron.* 85 (2016) 32–45, <https://doi.org/10.1016/j.bios.2016.04.091>.
- [12] A. Chen, S. Yang, Replacing antibodies with aptamers in lateral flow immunoassay, *Biosens. Bioelectron.* 71 (2015) 230–242, <https://doi.org/10.1016/j.bios.2015.04.041>.
- [13] N. Komarova, A. Kuznetsov, Inside the black box: what makes SELEX better? *Molecules* 24 (2019) 3598, <https://doi.org/10.3390/molecules24193598>.
- [14] M. Blind, M. Blank, Aptamer selection technology and recent advances, *Mol. Ther. Nucleic Acids* 4 (2015) e223, <https://doi.org/10.1038/mtna.2014.74>.
- [15] H. Sun, Y. Zu, A highlight of recent advances in aptamer technology and its application, *Molecules* 20 (2015) 11959–11980, <https://doi.org/10.3390/molecules200711959>.
- [16] Y. Song, J. Song, X. Wei, M. Huang, M. Sun, L. Zhu, B. Lin, H. Shen, Z. Zhu, C. Yang, Discovery of aptamers targeting the receptor-binding domain of the SARS-CoV-2 spike glycoprotein, *Anal. Chem.* 92 (2020) 9895–9900, <https://doi.org/10.1021/acs.analchem.0c01394>.
- [17] L. Jiuxing, Z. Zijie, G. Jimmy, S. Hannah D, A. Jann C, C. Alfredo, D.M.F. Carlos, M. Karen L, B. Cynthia, S. Bruno J, Y. Deborah, S. Leyla, M. Matthew S, B. John D, L. Yingfu, Diverse high-affinity DNA aptamers for wild-type and B.1.1.7 SARS-CoV-2 spike proteins from a pre-structured DNA library, *Nucleic Acids Res.* 49 (2021) 7267–7279, <https://doi.org/10.1093/nar/gkab574>.
- [18] M. Sun, S. Liu, X. Wei, S. Wan, M. Huang, T. Song, Y. Lu, X. Weng, Z. Lin, H. Chen, Y. Song, C. Yang, Aptamer blocking strategy inhibits SARS-CoV-2 virus infection, *Angew. Chem., Int. Ed. Engl.* 60 (2021) 10266–10272, <https://doi.org/10.1002/anie.202100225>.
- [19] X. Liu, Y. Wang, J. Wu, J. Qi, Z. Zeng, Q. Wan, Z. Chen, P. Manandhar, V. Cavener, N. Boyle, X. Fu, E. Salazar, S. Kuchipudi, V. Kapur, X. Zhang, M. Umetani, M. Sen, R. Willson, S. Chen, Y. Zu, Neutralizing aptamers block S/RBD-ACE2 interactions and prevent host cell infection, *Angew. Chem., Int. Ed. Engl.* 60 (2021) 10273–10278, <https://doi.org/10.1002/anie.202100345>.
- [20] A. Schmitz, A. Weber, M. Bayin, S. Breuers, V. Fieberg, M. Famulok, G. Mayer, A SARS-CoV-2 spike binding DNA aptamer that inhibits pseudovirus infection by an RBD-independent mechanism, *Angew. Chem., Int. Ed. Engl.* 60 (2021) 10279–10285, <https://doi.org/10.1002/anie.202100316>.
- [21] R. Liu, L. He, Y. Hu, Z. Luo, J. Zhang, A serological aptamer-assisted proximity ligation assay for COVID-19 diagnosis and seeking neutralizing aptamers, *Chem. Sci.* 44 (2020) 12157–12164, <https://doi.org/10.1039/d0sc03920a>.
- [22] H. Minagawa, K. Onodera, H. Fujita, T. Sakamoto, J. Akitomi, N. Kaneko, I. Shiratori, M. Kuwahara, K. Horii, I. Waga, Selection, characterization and application of artificial DNA aptamer containing appended bases with sub-nanomolar affinity for a salivary biomarker, *Sci. Rep.* 7 (2017) 42716, <https://doi.org/10.1038/srep42716>.
- [23] H. Minagawa, A. Shimizu, Y. Kataoka, M. Kuwahara, S. Kato, K. Horii, I. Shiratori, I. Waga, Fluorescence polarization-based rapid detection system for salivary biomarkers using modified DNA aptamers containing base-appended bases, *Anal. Chem.* 92 (2020) 1780–1787, <https://doi.org/10.1021/acs.analchem.9b03450>.
- [24] H. Minagawa, Y. Kataoka, M. Kuwahara, K. Horii, I. Shiratori, I. Waga, A high affinity modified DNA aptamer containing base-appended bases for human  $\beta$ -defensin, *Anal. Biochem.* 594 (2020), 113627, <https://doi.org/10.1016/j.ab.2020.113627>.
- [25] H. Minagawa, Y. Kataoka, H. Fujita, M. Kuwahara, K. Horii, I. Shiratori, I. Waga, Modified DNA aptamers for C-reactive protein and lactate Dehydrogenase-5 with sub-nanomolar affinities, *Int. J. Mol. Sci.* 21 (2020) 2683, <https://doi.org/10.3390/ijms21082683>.
- [26] F. Kato, S. Matsuyama, M. Kawase, T. Hishiki, H. Katoh, M. Takeda, Antiviral activities of mycophenolic acid and IMD-0354 against SARS-CoV-2, *Microbiol. Immunol.* 64 (9) (2020) 635–639, <https://doi.org/10.1111/1348-0421.12828>. Epub 2020 July 25.
- [27] M. Sasaki, K. Uemura, A. Sato, S. Toba, T. Sanaki, K. Maenaka, et al., SARS-CoV-2 variants with mutations at the S1/S2 cleavage site are generated in vitro during propagation in TMPRSS2-deficient cells, *PLoS Pathog.* 17 (1) (2021), e1009233, <https://doi.org/10.1371/journal.ppat.1009233>. Epub 2021/01/21.
- [28] S. Kato, T. Ono, H. Minagawa, K. Horii, I. Shiratori, I. Waga, K. Ito, T. Aoki, T. Aoki, FSBC: fast string-based clustering for HT-SELEX data, *BMC Bioinf.* 21 (2020) 263, <https://doi.org/10.1186/s12859-020-03607-1>.
- [29] I. Shiratori, J. Akitomi, D.A. Boltz, K. Horii, M. Furuichi, I. Waga, Selection of DNA aptamers that bind to influenza A viruses with high affinity and broad subtype specificity, *Biochem. Biophys. Res. Commun.* 443 (2014) 37–41, <https://doi.org/10.1016/j.bbrc.2013.11.041>.
- [30] O. Urs A, G. Louis S, G. Larry, J. Nebojsa, Systematic selection of modified aptamer pairs for diagnostic sandwich assays, *Biotechniques* 56 (2014) 125–133, <https://doi.org/10.2144/000114134>, eCollection 2014.
- [31] S. Strauss, P.C. Nickels, M.T. Strauss, V.J. Sabinina, J. Ellenberg, J.D. Carter, S. Gupta, N. Janjic, R. Jungmann, Modified aptamers enable quantitative sub-10-nm cellular DNA-PAINT imaging, *Nat. Methods* 15 (2018) 685–688.
- [32] D. Shangguan, Z. Tang, P. Mallikaratchy, Z. Xiao, W. Tan, Optimization and modifications of aptamers selected from live cancer cell lines, *Chembiochem* 8 (2007) 603–606, <https://doi.org/10.1002/cbic.200600532>.
- [33] X. He, L. Guo, J. He, H. Xu, J. Xie, Stepping library-based post-SELEX strategy approaching to the minimized aptamer in SPR, *Anal. Chem.* 89 (2017) 6559–6566, <https://doi.org/10.1021/acs.analchem.7b00700>.
- [34] R. Lorenz, S.H. Bernhart, C.H.Z. Siederdisen, H. Tafer, C. Flamm, P.F. Stadler, I.L. Hofacker, ViennaRNA package 2.0, *Algorithm Mol. Biol.* 6 (2011), <https://doi.org/10.1186/1748-7188-6-26>.
- [35] J. Lan, J. Ge, J. Yu, S. Shan, H. Zhou, S. Fan, Q. Zhang, X. Shi, Q. Wang, L. Zhang, X. Wang, Structure of the SARS-CoV-2 spike receptor-binding domain bound to the ACE2 receptor, *Nature* 581 (2020) 215–220, <https://doi.org/10.1038/s41586-020-2180-5>.
- [36] V. Tragni, F. Preziosi, L. Laera, A. Onofrio, S. Todisco, M. Volpicella, A.D. Grassi, C.L. Pierri, A modular molecular framework for quickly estimating the binding affinity of the spike protein of SARS-CoV-2 variants for ACE2, in presence of mutations at the spike receptor binding domain, *bioRxiv* (2021), <https://doi.org/10.1101/2021.05.26.445422>. May 26.
- [37] P. Kerpedjiev, S. Hammer, I.L. Hofacker, Forna (force-directed RNA): simple and effective online RNA secondary structure diagrams, *Bioinformatics* 31 (2015) 3377–3379, <https://doi.org/10.1093/bioinformatics/btv372>.